International Journal of Thermophysics, Vol. 20, No. 1, 1999

Rayleigh–Taylor-Like Instability in Near-Critical Pure Fluids[1]

B. Zappoli,[2] S. Amiroudine,[3,4] and S. Gauthier[5]

The hydrodynamic stability of a thermodiffusive interface in a near-supercritical fluid is studied. The Navier-Stokes equations written for a van der Waals gas above its critical point are solved by means of a finite volume numerical method. The growth rate of the fluctuations shows that there exists a cutoff wave number beyond which the short wavelengths are stabilized by diffusion. The good agreement between the obtained values and recent theories for miscible fluids confirms that a near-critical fluid subjected to a thermal gradient may develop a gravitational instability for which the density gradient is driven by thermal diffusion and large compressibility.

KEY WORDS: finite volume methods; numerical hydrodynamics; Rayleigh–Taylor instability; supercritical fluids.

1. INTRODUCTION

The weak diffusivity of near-critical pure fluids and their large compressibility lead to very specific mechanisms of thermal homogenization. The piston effect, which is of a thermoacoustic nature, allows for a very fast thermal homogenization under zero gravity conditions although the thermal diffusivity is very small [1–4]. Under normal gravity conditions and for a side-heated square-shaped cavity, we have recently shown that this mechanism is still responsible for heat equilibration [5]. We are interested

[1] Paper presented at the Thirteenth Symposium on Thermophysical Properties, June 22–27, 1997, Boulder, Colorado, U.S.A.

[2] Centre National d'Etudes Spatiales, CNES/DP/MP/SC, 18 Av. E. Belin, 31401 Toulouse Cedex 04, France.

[3] Université des Antilles et de la Guyane, Faculté des Sciences, Département de Physique, 97159 Pointe à Pitre, Guadeloupe, French West Indies.

[4] To whom correspondence should be addressed.

[5] CEA/Limeil-Valenton, 94195 Villeneuve-St-Georges, Cedex, France.

0195-928X/99/0100-0257$16.00/0

here in a different situation, although it is also linked with the storage of cryogens and more generally to the stability of diffusion fronts in miscible fluids.

When one performs the numerical modeling of a bottom-heated cavity filled with a supercritical fluid (Rayleigh–Benard configuration), the lateral walls of which are insulated while the top wall is thermostated at the initial temperature, thermal plumes arise at the bottom wall. As the bulk fluid is homogeneously heated by the piston effect, a cooling thermal boundary layer forms along the upper wall [6]. This layer of fluid is heavier than the fluid located below and thus gives birth to droplets as shown in Fig. 1. The mechanism of formation of these droplets looks like a Rayleigh–Taylor instability. We thus oriented our investigations towards a front diffusion instability, analogous to the one encountered in miscible fluids [7–10]. We have considered a simpler situation (see Fig. 2) in which the upper half of a square-shaped isobaric cavity of infinite extension filled with a near-supercritical fluid at rest is some mK cooler than the bottom half. The top and bottom walls are at constant initial temperature. The aim of this work is to perform a numerical stability analysis of the thermal diffusion interface which is present between the two halves of the cavity. To this end, we use a technique which consists of studying the dynamics of growth of fluctuations of a fluid property at the interface.

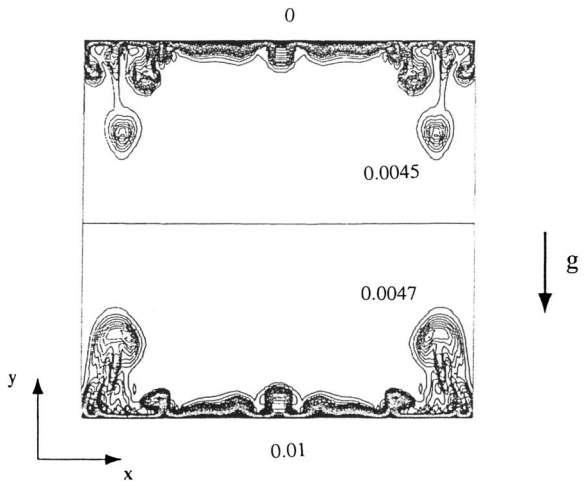

Fig. 1. Temperature difference $(T' - T'_0)$ in K for a square-shaped cavity heated from below initially at 1 K from the critical point and 8.3 s after a 10 mK increase in temperature, from Ref. 6.

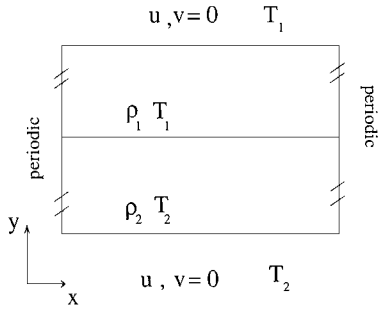

Fig. 2. The two-dimensional model.

2. MATHEMATICAL MODEL

The model is identical to the one used in Ref. 5, and is merely repeated here. The Navier–Stokes equations are those describing a Newtonian, viscous and hypercompressible pure fluid. For the equation of state, we have chosen to use the van der Waals equation, although it is well known that it does not correctly describe the critical coordinates, namely it leads neither to the correct critical pressure nor to the correct critical exponents (i.e., the exponents describing the critical divergence of transport properties). If necessary, i.e., when close enough to the critical point or for comparisons with experimental results, it is possible to use the restricted cubic model of Ref. 11.

Pressure is normalized with respect to that for an ideal gas at critical conditions. The other variables are referenced to their critical values. The governing equations are written in the following form:

$$\frac{\partial \rho}{\partial t} + \nabla \cdot (\rho \mathbf{v}) = 0 \tag{1}$$

$$\frac{D(\rho \mathbf{v})}{Dt} = -\gamma^{-1} \nabla P + \varepsilon \left[\nabla^2 \mathbf{v} + \frac{1}{3} \nabla(\nabla \cdot \mathbf{v}) \right] + \frac{1}{F_r} \rho \mathbf{g} \tag{2}$$

$$\frac{D(\rho T)}{Dt} = -(\gamma - 1)(P + a\rho^2)(\nabla \cdot v) \frac{\varepsilon \gamma}{P_r} \nabla \cdot [\lambda \nabla T] + \Phi \tag{3}$$

where $\Phi = \varepsilon\gamma(\gamma - 1)[v_{i,j} v_{j,i} + v_{i,j} v_{i,j} - \frac{2}{3} v_{i,i} v_{j,j}]$ is the viscous dissipation rate and ε is a small parameter defined by $\varepsilon = P_r t'_a / t'_d$, where $t'_d = L'^2 / \kappa'_0$ is the characteristic heat diffusion time for the ideal gas (L' is the characteristic length and κ'_0 is the thermal diffusivity) and $t'_a = L'/c'_0$ is the characteristic time of acoustic phenomena [$c'_0 = (\gamma R' T'_c)^{1/2}$ represents the sound

velocity]. It must be noted that t'_d is not the characteristic time for diffusion in a supercritical fluid. Taking into account the vanishing thermal diffusivity of near-critical fluids, this characteristic time would be of order $t'_d/\Delta T^{1/2}$, which is even longer.

The quantity $P_r = v'_0/\kappa'_0$ is the Prandtl number (where v'_0 is the kinematic viscosity) and $F_r = c'_0/L'g'_0$ is the acoustic Froude number (L' is the characteristic length, g'_0 is the acceleration of gravity, and c'_0 is the sound velocity). Ail the zero subscripts represent properties for an ideal gas. The following thermal and transport coefficients are considered:

$$\lambda = 1 + \Lambda(T-1)^{-0.5}; \qquad C_v = 1; \qquad \tilde{\mu} = 1$$

where λ, C_v, and $\tilde{\mu}$ are, respectively, the heat conductivity, the specific heat at constant volume, and the dynamic viscosity relative to their ideal gas values. The van der Waals equation can be written in the following nondimensional form:

$$P = \frac{\rho T}{1-b\rho} - a\rho^2 \tag{4}$$

where $a = 9/8$ and $b = 1/3$ are given by the expression of the critical coordinates.

The fluid is initially at rest, and stratification is neglected since the distance to the critical point is greater than 1 K. The initial conditions for the upper layer are

$$\begin{cases} \rho_1 = 1; \quad T_1 = 1 + \Delta T; \quad P_1 = (1+\Delta T)/(1-b) - a \\ u = v = 0 \end{cases} \qquad \text{for} \quad y \in [0.5, 1]$$

where $(T'_1 - T'_c)/T'_c = \Delta T \ll 1$, and T'_1 and T'_c are, respectively, the initial and critical temperatures; the variables with a prime have dimensions. For the lower layer, the initial conditions are such that the density is given while the temperature is determined in such a way that the pressure is homogeneous within the whole cavity:

$$\begin{cases} \begin{cases} \rho_2 = 1 - \Delta\tilde{\varepsilon}; \qquad T_2 = \left[\dfrac{\rho_1 T_1}{1-b\rho_1} + a(\rho_2^2 - \rho_1^2)\right] \dfrac{(1-b\rho_2)}{\rho_2}; \qquad P_2 = P_1 \\ u = v = 0 \end{cases} \\ \qquad \text{for} \quad y \in [0, 0.5] \end{cases}$$

where $\Delta\tilde{\varepsilon}$ corresponds to the given density difference between the two layers. On the horizontal walls, the following boundary conditions are considered:

$$\begin{cases} u = v = 0 \\ T(x, 0, t) = T_2;\ T(x, 1, t) = T_1 \end{cases}$$

Periodic conditions are considered on lateral boundaries, i.e., for any field variable ϕ (temperature, velocity), the following relation holds at all times:

$$\phi(0, y, t) = \phi(\tilde{\lambda}, y, t)$$

where $\tilde{\lambda}$ represents the wavelength of the initial perturbation, the dynamics of which are to be studied. When the thermal constraint is suppressed, thermal diffusion which is the driving force of the evolution begins to operate. As density is related to temperature via the equation of state, a diffusive interface forms which is similar to the one which would form between two miscible liquids. The fluctuations whose dynamics are to be studied are introduced with the form of an initial nonzero velocity written as

$$v(x, y = 0.5, t = 0) = A \cos\left(\frac{2\pi}{\tilde{\lambda}} x\right) \tag{5}$$

where A is the amplitude of the perturbation ($A = 10^{-2}$).

3. NUMERICAL METHOD

The governing equations are numerically solved by a finite-volume method with a SIMPLER-type algorithm [12, 13]. The numerical scheme is of first order in time, and the discretization in space uses the power lower scheme [12]. A nonuniform staggered grid is used to take into account the presence of huge initial gradients at the interface. The grid is uniform in the x direction. The acoustic filtering procedure is used to reduce computational time [5, 13], and the calculations are performed on the piston effect time scale (which is between the acoustic and the diffusion times defined in Section 2); on that time scale, the pressure can be separated into two parts, one of which is homogeneous in space plus a small nonhomogeneous acoustic perturbation which can be filtered at first order. The dynamics of the growth of the fluctuations, that is to say, the determination of rate of growth $\sigma(k)$, where k is the wave number of the initial perturbation, is determined in the following way: after sampling two values of a field variable (the velocity, for example) at a grid point for two different times

t_1 and t_2, one determines $\sigma(k)$ in expressing the velocity as an exponential function of time,

$$\begin{cases} v_1 = A_1 e^{\sigma t_1} \\ v_2 = A_2 e^{\sigma t_2} \end{cases}$$

from which one can extract $\sigma(t, k)$

$$\sigma = \frac{\ln(A_1/A_2)}{t_1 - t_2} \tag{6}$$

The value of $\sigma(k)$ which corresponds to the linear regime under study is considered to be the one corresponding to the plateau zone of the time history of $\sigma(t)$ for which A_1 and A_2 are independent of time.

4. RESULTS AND DISCUSSION

The calculations are performed for a cavity filled with CO_2 at critical density, the temperature of the upper part of which is 1 K above the critical temperature. This value determines the value of the transport coefficients, the other variations being only perturbations. The density difference between the upper and lower parts of the cavity is directly related to the temperature difference and compressibility. Two nondimensional density differences are studied: $\Delta\tilde{\varepsilon} = 10^{-2}$ and 10^{-3} and they correspond, respectively, to temperature differences of 15.2 and 1.49 mK. The values of the kinematic viscosity and thermal diffusivity at 1 K above the critical point are $v = 4.48 \times 10^{-4}\,\mathrm{cm^2 \cdot s^{-1}}$ and $\kappa = 0.86 \times 10^{-4}\,\mathrm{cm^2 \cdot s^{-1}}$.

The values of $\sigma(k)$ are shown on Fig. 3. One can point out first that there exists a cutoff wave number beyond which the small wavelengths are damped by diffusion. This is in agreement with the conclusions of recent work [7, 9, 15], which, taking into account both viscosity and diffusion, make it necessary for a cutoff wave number to be equal to [9]:

$$\tilde{\lambda}_c = 2\pi \left(\frac{16vD}{3gR} \right)^{1/3} \tag{7}$$

where D is the interdiffusion coefficient for miscible fluids (which is replaced, in our case, by the thermal diffusion coefficient), g is the acceleration of gravity, and $R = (\rho_1 - \rho_2)/(\rho_1 + \rho_2)$. Table I compares the cutoff values obtained by the present numerical simulations with the ones deduced from the above formulas.

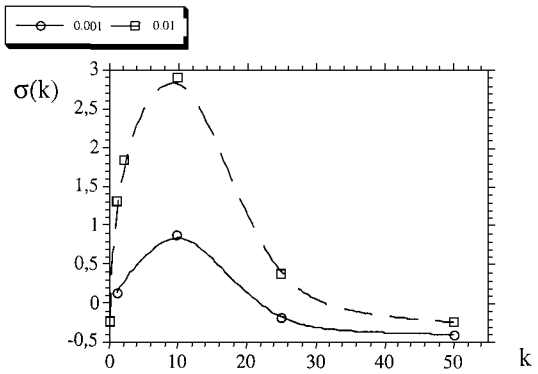

Fig. 3. Instability growth rate as a function of the wave number for $\Delta\rho = 0.01$ ($4.678\ \mathrm{kg \cdot m^{-3}}$) and $\Delta\rho = 0.001$ ($0.4678\ \mathrm{kg \cdot m^{-3}}$); the initial temperature is 1 K above the critical point.

Figure 4 shows the temperature field at a given time ($t' = 1$ s) for an initial perturbation wavelength $\tilde{\lambda} = 0.1$ that gives a high growth rate. It must be emphasized here that the values of the Schmidt number for the critical fluid are of order 10, whereas they are of order 10^3 for normal miscible liquids. This is due to the strong decrease of the kinematic viscosity; the thermal diffusivity of the critical fluid, although weak for a gas, is two orders of magnitude higher than mass diffusion in miscible liquids. The length scale associated with the micro-drops formed by the instability is thus small and it appears that the thermal homogenization process of a supercritical fluid on ground may undergo a micro-mixing phase: micro-drops are formed that then relax by diffusion. The measured homogenization time may thus appear much smaller than the one calculated on the cell length scale. The present calculations need to be completed by a systematic study as a function of the distance to the critical point as well as by a linear stability analysis [16].

Table I. Cutoff Wavelength as a Function of Density Difference

	$\tilde{\lambda}_c$ (mm)	
$\Delta\rho$ ($\mathrm{kg \cdot m^{-3}}$)	Kurowski et al. [9]	Numerical
4.678	0.258	0.280
0.4678	0.557	0.434

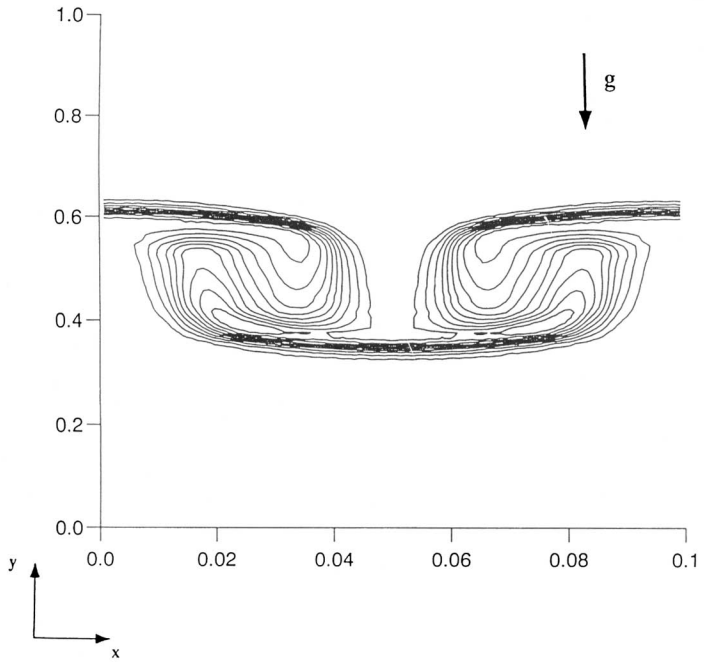

Fig. 4. Temperature difference 1 s after the thermal constraint has been suppressed (the wavelength of the initial perturbation is $\tilde{\lambda}' = 1$ mm).

REFERENCES

1. B. Zappoli, D. Bailly, Y. Garrabos, B. Le Neindre, P. Guenoun, and D. Beysens, *Phys. Rev. A* **41**:2224 (1990).
2. A. Onuki, H. Hong, and R. A. Ferrel, *Phys. Rev. A* **41**:2256 (1990).
3. H. Boukari, R. L. Pego, and R. W. Gammon, *Phys. Rev. A* **41**:2260 (1990).
4. P. Guenoun, D. Beysens, B. Khalil, Y. Garrabos, B. Kammoun, B. Le Neindre, and B. Zappoli, *Phys. Rev. E* **47**:1531 (1993).
5. B. Zappoli, S. Amiroudine, P. Carles, and J. Ouazzani, *J. Fluid Mech.* **316**:53 (1996).
6. S. Amiroudine, P. Larroudé, P. Bontoux, and B. Zappoli, *Proc. Second Eur. Symp. "Fluids in Space"* (Naples, Italy, 1996).
7. F. Brochard and P. G. De Gennes, *C. R. Acad. Sci.* **318**(II):27 (1994).
8. J. R. Authelin, F. Brochard, and P. G. De Gennes, *C. R. Acad. Sci.* **317**(II):1539 (1993).
9. P. Kurowski, C. Misbah, and S. Tchourkine, *Eur. Phys. Lett.* **29**:309 (1995).
10. D. H. Sharp, *Physica D* **12**:3 (1984).
11. M. R. Moldover, J. V. Sengers, R. W. Gammon, and R. J. Hocken, *Rev. Mod. Phys.* **51**:79 (1979).
12. S. V. Patankar, *Numerical Heat Transfer and Fluid Flow* (Hemisphere, New York, 1980).

13. S. Amiroudine, *Modélisation numérique des phénomènes de transport de chaleur et de masse dans les fluides supercritiques*, Ph.D. dissertation (Institut de Recherche sur les Phénomènes Hors-Equilibre, Marseille, 1995).
14. B. Zappoli and P. Carles, *Physica D* **89**:381 (1996).
15. F. Renaud and S. Gauthier, personal communication (1995).
16. S. Chandrasekhar, *Hydrodynamic and Hydromagnetic Stability* (Clarendon Press, Oxford, 1961).